THE UNIVERSITY OF ALABAMA® | University Libraries

Perpendicular Magnetic Tunnel Junctions Using Co-based Multilayers

T. Mewes – University of Alabama

et al.

Deposited 08/30/2018

Citation of published version:

Tadisina, Z., et al. (2010): Perpendicular Magnetic Tunnel Junctions Using Co-based Multilayers, *Journal of Applied Physics*, 107. https://doi.org/10.1063/1.3358242

© 2010 American Institute of Physics

Perpendicular magnetic tunnel junctions using Co-based multilayers

Z. R. Tadisina, A. Natarajarathinam, B. D. Clark, A. L. Highsmith, T. Mewes, S. Gupta, E. Chen, and S. Wang

Citation: Journal of Applied Physics **107**, 09C703 (2010); doi: 10.1063/1.3358242
View online: https://doi.org/10.1063/1.3358242
View Table of Contents: http://aip.scitation.org/toc/jap/107/9
Published by the American Institute of Physics

Articles you may be interested in

Ultrathin Co/Pt and Co/Pd superlattice films for MgO-based perpendicular magnetic tunnel junctions
Applied Physics Letters **97**, 232508 (2010); 10.1063/1.3524230

Magnetic tunnel junctions with Co-based perpendicular magnetic anisotropy multilayers
Journal of Vacuum Science & Technology A: Vacuum, Surfaces, and Films **28**, 973 (2010); 10.1116/1.3430549

Spin torque switching of perpendicular $\mathrm{Ta}|\mathrm{CoFeB}|\mathrm{MgO}$-based magnetic tunnel junctions
Applied Physics Letters **98**, 022501 (2011); 10.1063/1.3536482

Tunnel magnetoresistance of 604% at $300K$ by suppression of Ta diffusion in $\mathrm{CoFe}B/\mathrm{Mg}O/\mathrm{CoFe}B$ pseudo-spin-valves annealed at high temperature
Applied Physics Letters **93**, 082508 (2008); 10.1063/1.2976435

Very strong antiferromagnetic interlayer exchange coupling with iridium spacer layer for perpendicular magnetic tunnel junctions
Applied Physics Letters **110**, 092406 (2017); 10.1063/1.4977565

Enhancement of perpendicular magnetic anisotropy through reduction of Co-Pt interdiffusion in (Co/Pt) multilayers
Applied Physics Letters **100**, 142410 (2012); 10.1063/1.3701585

Perpendicular magnetic tunnel junctions using Co-based multilayers

Z. R. Tadisina,[1] A. Natarajarathinam,[1] B. D. Clark,[1] A. L. Highsmith,[1] T. Mewes,[1] S. Gupta,[1,a)] E. Chen,[2] and S. Wang[2]
[1]*MINT Center, University of Alabama, Box 870209, Tuscaloosa, Alabama 35487, USA*
[2]*Grandis, 1123 Cadillac Court, Milpitas, California 95035, USA*

(Presented 21 January 2010; received 11 November 2009; accepted 2 December 2009; published online 21 April 2010)

CoFeB/MgO/CoFeB magnetic tunnel junctions (MTJs) with perpendicular magnetic anisotropy (PMA) free and reference layers composed of Co/M (where M=Pd or Ni) multilayers have been optimized for high PMA and high tunneling magnetoresistance (TMR). The effects of Co thickness, Pd thickness, and the number of Co/Pd bilayers on the anisotropy and coercivity of the $[Co/Pd]_n$ multilayer films have been studied for both free and reference layers. The damping parameter α of CoFeB capped multilayers was determined using broadband ferromagnetic resonance. The transport properties of the patterned MTJ stacks were measured from 10 to 400 K. A maximum TMR of 10% at 10 K (5%–10% at 300 K) was obtained for these perpendicular MTJs, regardless of whether or not they were magnetically annealed for MgO–CoFeB crystallization. This indicates that the fcc-bcc-fcc transitions from the fcc multilayers to the bcc CoFeB/MgO/CoFeB do not promote the "giant MgO TMR effect" caused by symmetry filtering. © *2010 American Institute of Physics*. [doi:10.1063/1.3358242]

I. INTRODUCTION

Magnetic tunnel junctions (MTJs) with perpendicular magnetic anisotropy (PMA) materials have been extensively studied for applications such as high density read heads and magnetoresistive random access memory (MRAM).[1–5] The phenomenon of spin transfer (ST) switching applied to MTJs with PMA has generated considerable interest in applications such as spin torque transfer random access memory (STT-RAM).[1] In order to have high density MRAM, the MTJ cell size should be very small, which works in favor of STT-RAM, because the switching current scales down as the MTJ size shrinks. The low switching current and large thermal stability factors are the two important issues for realizing high density STT-MRAM. The theoretical expressions predict that lower critical currents for switching and high thermal stability can be achieved by using PMA materials.[1]

The thermal stability factor Δ is expressed as

$$\Delta = \frac{KV}{k_B T}. \tag{1}$$

where K is the anisotropy, V is the volume, k_B is Boltzmann's constant, and T is the absolute temperature.

The critical current I_C can be expressed as[6]

$$I_C = \frac{2e}{\hbar}\frac{\alpha}{\eta} M_S V \cdot H_{\text{eff}}, \tag{2}$$

where α is the Gilbert damping coefficient, η is the ST efficiency factor (maximum value=1), and H_{eff} is an effective field, which for in-plane material is

$$H_{\text{eff}} = H_K + 2\pi M_S. \tag{3}$$

and the effective field is dominated by the shape anisotropy term.

For PMA materials with an out-of-plane anisotropy $H_{K\perp} > 4\pi M_S$, the effective field is

$$H_{\text{eff}} = H_{K\perp} - 4\pi M_S. \tag{4}$$

Thus, in PMA-based MTJs the barrier that determines the thermal stability also determines the critical current. In contrast, for the in-plane tunnel junction, the switching current has to overcome the additional demagnetizing field, but the thermal stability is determined by the in-plane anisotropy. Therefore, perpendicular anisotropy materials can have an advantage over in-plane devices[7] provided that one can maintain the same ratio of (α/η). This shows the importance of damping studies in out-of-plane materials as presented in this article. The thermal stability factor is directly proportional to the volume of the memory cell and the magnetic anisotropy, so when the cell size is reduced, materials with large magnetic anisotropy are required. Generally, PMA materials have larger magnetic anisotropy than conventional in-plane magnetic materials such as NiFe and CoFeB.

In this paper, we have studied the PMA of Co/M (Refs. 7–12) (where M=Ni, Pd) multilayer (ML) systems as a function of bilayer thickness, bilayer ratio, and the number of bilayers.

II. EXPERIMENTAL DETAILS

A series of Co/M (where M=Ni, Pd) MLs is deposited on (100) silicon substrates in a seven-target SFI Shamrock planetary sputtering system using dc magnetron sputtering for all the layers. The sputtering system was pumped down to a base pressure of less than 8×10^{-8} Torr (2.4×10^{-6} Pa). Deposition powers ranged from 250 to 450 W,

a)Electronic mail: sgupta@eng.ua.edu.

 © 2010 American Institute of Physics

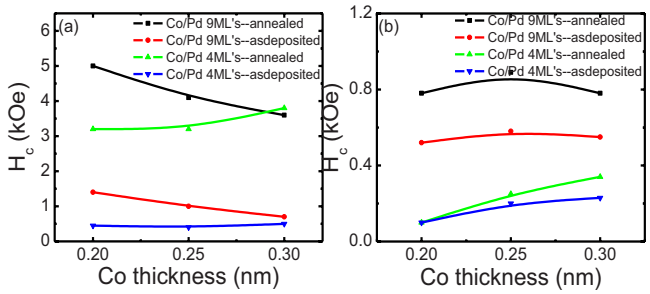

FIG. 1. (Color online) Coercivity vs thickness of Co in Co/Pd MLs for (a) Co/Pd as-deposited and annealed MLs deposited below the MgO barrier layer and (b) Co/Pd as-deposited and annealed MLs deposited above the MgO barrier layer.

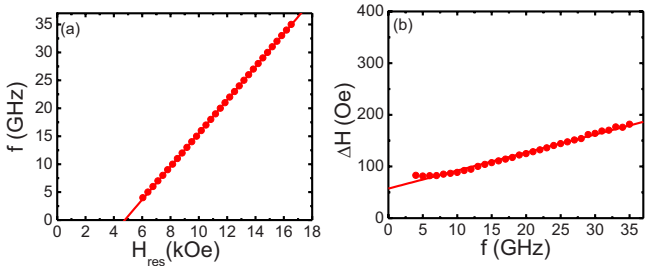

FIG. 2. (Color online) Frequency dependent FMR data of Pd seed/[Co0.2/Pd1]*9/Co0.3/CoFeB2/MgO3 stack with the field applied along the out-of-plane direction: (a) frequency vs H_{res} and (b) ΔH vs frequency.

corresponding to deposition rates of 0.6–1.8 nm/s. Deposition pressures were held at 2 mTorr (0.26 Pa). A combination of Ta/Pt or Ta/Pd was used as seed layers to promote the fcc (111) texture of the magnetic MLs and a capping layer of Ru/Ta was used to protect the MLs from oxidation. The magnetic and structural properties of the as-deposited samples were characterized by alternating gradient magnetometry, x-ray diffraction, stress measurements, and local electrode atom probe.[8] The damping parameter α and effective magnetization were measured using a customized, fully automated broadband variable temperature ferromagnetic resonance (FMR) capability using coplanar waveguides with a frequency range of 2–50 GHz.

III. RESULTS AND DISCUSSION

We have investigated PMA in Co/Pd MLs,[9,10] as well as Co/Ni MLs.[11–13] The magnetic anisotropy in Co/Pd MLs can be easily tailored by changing the thickness of the individual Co and Pd layers. We carried out a detailed study of these MLs, varying individual layer thicknesses, Co/Pd ratios, and the number of MLs before and after annealing. It was observed that Co/Pd MLs grown above MgO were lower in coercivity than those grown below MgO, with PMA observed for MLs grown above and below MgO. These Co/Pd MLs can be used as pinned and free layers in pseudo-MTJs if they have a clear difference in coercivities. The thickness of the ferromagnetic Co layer was varied from 0.2 to 0.3 nm, keeping the Pd thickness constant at 1 nm. These Co/Pd MLs, when grown on Ta 5 nm/Pt 10 nm seed layers showed very high coercivity for both four and nine MLs; moreover, the coercivity increased dramatically upon annealing these samples, as shown in Fig. 1(a). However, if MgO is used as a seed layer, the coercivity decreases for both as-deposited and annealed samples, as shown in Fig. 1(b).

PMA is observed in all the Co/Pd MLs below and above the MgO barrier layer. The remanent magnetization perpendicular to the film plane is almost identical to the saturation magnetization value, indicating square loops. Our preliminary optimization study led to a MTJ design in which we deposited nine and four MLs of Co/Pd below and above the MgO barrier layer for the reference and free layers, respectively.

We have performed frequency dependent FMR measurements on Co/Pd MLs with CoFeB on top of these MLs to investigate the amount of CoFeB that can be pulled out of the film plane. To quantify this, we determined the effective magnetization M_{eff} with $4\pi M_{\text{eff}}=4\pi M_S-H_{K\perp}$ by fitting the frequency data to the Kittel formula[14] with the fields ranging up to 17 kOe applied along the out-of-plane direction to ensure saturation, as shown in Fig. 2. Figure 3 shows M_{eff} values for different thicknesses of CoFeB and it is clear that as the thickness of the CoFeB on top of these MLs increases, M_{eff} changes from negative to positive values, indicating a shift from PMA to the in-plane behavior. Specifically, a 0.9 nm thick CoFeB is pulled out of plane by the Co/Pd MLs, but at higher thicknesses, CoFeB goes in-plane. The negative M_{eff} indicates that the magnetization points out of the film plane. However, the observed resonance is most likely due to CoFeB on top of these MLs, which is also consistent with the strong dependence of M_{eff} on the thickness of CoFeB and the lack of an observable resonance for Co/Pd MLs without CoFeB. The Gilbert damping parameter α is obtained by fitting the measured frequency dependence of the linewidth ΔH to the following formula:[15]

$$\Delta H = \Delta H_0 + \frac{2}{\sqrt{3}}\frac{\alpha}{\gamma}\omega. \tag{5}$$

The damping parameter α increases with decreasing CoFeB thickness, as seen in Fig. 3(b). One plausible origin for this is spin pumping, which should scale with the inverse thickness of CoFeB.[16,17]

These PMA-based materials were deposited as full MTJ stacks with the structure: seed layer/$[\text{Co0.2/Pd1}]_9$/CoFeB0.4/MgO1.6/CoFeB0.4/$[\text{Co0.3/Pd1}]_4$/cap. These full MTJ stacks were characterized by magnetometry to ensure coercivity differences between the free and the reference layers, as shown in Fig. 4 for Co/Pd MLs under perpendicu-

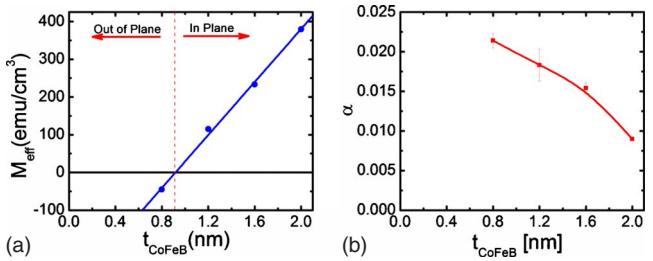

FIG. 3. (Color online) (a) M_{eff} vs thickness of CoFeB deposited on top of [Co0.2/Pd1]*9 MLs. (b) Damping constant vs thickness of CoFeB deposited on top of [Co0.2/Pd1]*9 MLs.

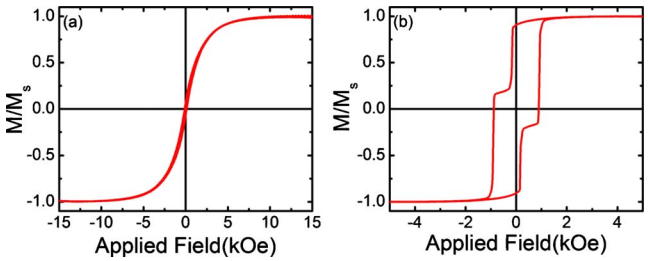

FIG. 4. (Color online) *MH* loops of perpendicular MTJ with Co/Pd MLs as free and reference layers: (a) in-plane loop and (b) out-of-plane loop. The MTJ stack is Pd(seed layer)/$(Co0.2/Pd1)_9$/CoFeB0.4/MgO1.6/CoFeB0.4/$(Co0.3/Pd1)_4$/Ru(cap).

lar applied fields. It can be seen that the loop shows clear perpendicular anisotropy and the coercivities of the pinned layer and free layer are distinct.

These stacks were then patterned into MTJ devices using a stepwise planarization technique developed by us at UA. This technique repeatedly uses a specific sequence of processing steps—pattern, etch, deposit, and lift-off—in such a way that the device is kept planar at each critical phase of its fabrication. The critical aspect of this procedure is that the etch depth and the deposition thickness must match so that the sample will be planar after the lift-off procedure. Figures 5(a) and 5(b) show field-switched transport characteristics at 100 K for the preliminary micron-sized devices fabricated using (a) Co/Pd MLs for free and reference layers and (b) Co/Pd ML reference layer and Co/Ni bottom free layer. These samples are annealed at 300 °C for 2 h with an out-of-plane applied field of 5 kOe. The field switching characteristics of the Co/Pd ML device is excellent. The seed used for the Co/Ni ML was Cu, which is not as effective as Pt in promoting fcc (111) texture, and hence PMA, which explains why the free layer switching is not as sharp as the Co/Pd reference layer switching.

IV. CONCLUSIONS

In conclusion, we have optimized various types of PMA magnetic multilayered stacks using different seed layers. The coercivity and out-of-plane anisotropy of these MLs have been optimized. FMR measurements were performed to obtain the M_{eff} and damping constant values. These multilayered combinations were used as free and pinned layers in MTJs and excellent switching characteristics were seen. However, the TMR values obtained are small (~10%) compared to MgO-based in-plane MTJs reported in literature. We believe that the fundamental problem in not obtaining TMR values greater than 10% is caused by the lattice mismatch between the fcc (111) PMA MLs and the MgO/CoFeB bcc (001) layers, combined with the necessarily thin (~0.5 nm) layers of CoFeB used in these junctions to maintain perpendicular anisotropy.

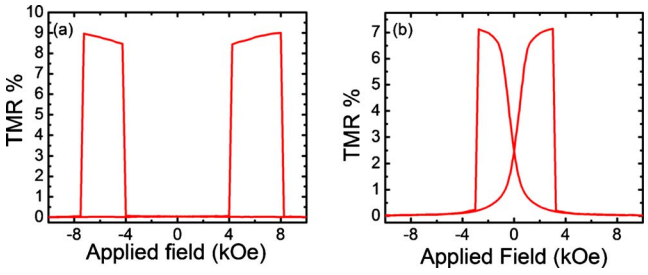

FIG. 5. (Color online) *MR* loops of (a) Co/Pd free and pinned layer and (b) Co/Pd pinned and Co/Ni free layer MTJs at 100K.

ACKNOWLEDGMENTS

This work was partially supported by the U.S. Department of Defense DARPA-MTO STT-RAM Universal Memory contract and Grandis Technology, Milpitas. Professor Patrick LeClair is acknowledged for his advice and support on the PPMS measurements. Professor W. H. Butler and Dr. C. Mewes are acknowledged for their elucidation of the theoretical concepts underlying this research effort.

[1] S. Mangin, D. Ravelosona, J. A. Katine, M. J. Carey, B. D. Terris, and E. E. Fullerton, Nature Mater. **5**, 210 (2006).
[2] N. Nishimura, T. Hirai, A. Koganei, T. Ikeda, K. Okano, Y. Sekiguchi, and Y. Osada, J. Appl. Phys. **91**, 5246 (2002).
[3] X. Zhu and J. G. Zhu, IEEE Trans. Magn. **42**, 2739 (2006).
[4] A. X. C. Cabrera, C. H. Chang, C. C. Hsu, M. C. Weng, C. C. Chen, C. T. Chao, J. C. Wu, Y. H. Chang, and T.-H. Wu, IEEE Trans. Magn. **43**, 914 (2007).
[5] M. Nakayama, T. Kai, N. Shimomura, M. Amano, E. Kitagawa, T. Nagase, M. Yoshikawa, T. Kishi, S. Ikegawa, and H. Yoda, J. Appl. Phys. **103**, 07A710 (2008).
[6] J. A. Katine and E. E. Fullerton, J. Magn. Magn. Mater. **320**, 1217 (2008).
[7] J. Shi, S. Tehrani, and M. R. Scheinfein, Appl. Phys. Lett. **76**, 2588 (2000).
[8] Z. Tadisina, A. Natarajarathinam, and S. Gupta, J. Vac. Sci. Technol. A (in press).
[9] D. Lim, S. Kim, and S. R. Lee, J. Appl. Phys. **97**, 10C902 (2005).
[10] K. Nakamura, S. Tsunashima, S. Iwata, and S. Uchiyama, IEEE Trans. Magn. **MAG-25**, 3758 (1989).
[11] F. J. A. den Broeder, E. Janssen, W. Hoving, and W. B. Zeper, IEEE Trans. Magn. **28**, 2760 (1992).
[12] G. H. O. Daalderop, P. J. Kelly, and M. F. H. Schuurmans, Phys. Rev. B **42**, 7270 (1990).
[13] G. H. O. Daalderop, P. J. Kelly, and F. J. A. den Broeder, Phys. Rev. Lett. **68**, 682 (1992).
[14] C. Kittel, Phys. Rev. **73**, 155 (1948).
[15] B. Heinrich, J. F. Cochran, and R. Hasegawa, J. Appl. Phys. **57**, 3690 (1985).
[16] Y. Tserkovnyak, A. Brataas, and G. E. W. Bauer, Phys. Rev. Lett. **88**, 117601 (2002).
[17] H. Lee, L. Wen, M. Pathak, P. Janssen, P. LeClair, C. Alexander, C. K. A. Mewes, and T. Mewes, J. Phys. D: Appl. Phys. **41**, 215001 (2008).